

M agnetic ordering in a doped frustrated spin-Peierls system

Nicolas Laurencie,¹ Didier Poilblanc,² and Anders W. Sandvik³

¹Laboratoire de Physique Théorique, CNRS-UMR 5152 Université Paul Sabatier, F-31062 Toulouse, France

²Laboratoire de Physique Théorique (CNRS-UMR 5152),
Université Paul Sabatier, F-31062 Toulouse, France

³Department of Physics, Åbo Akademi University, Porthansgatan 3, FIN-20500 Turku, Finland
(Dated: April 14, 2024)

Based on a model of a quasi-one dimensional spin-Peierls system doped with non-magnetic impurities, an effective two-dimensional Hamiltonian of randomly distributed $S=1/2$ spins interacting via long-range pairwise interaction is studied using a stochastic series expansion quantum Monte Carlo method. The susceptibility shows Curie-like behavior at the lowest temperatures reached although the staggered magnetisation is found to be finite for $T \rightarrow 0$. The doping dependence of the corresponding three-dimensional Neel temperature is also computed.

PACS numbers: 75.10.-b, 71.27.+a, 75.50.Ee, 75.40.Mg

Quasi one-dimensional (1D) quantum antiferromagnets exhibit fascinating magnetic properties at low temperatures. Some inorganic compounds, such as the germanate oxide CuGeO_3 ¹ and the vanadate oxide LiV_2O_5 ² are excellent realizations of weakly interacting frustrated spin-1/2 chains. A spin-Peierls (SP) transition to a gapped dimerised ground state (GS) has been seen experimentally in CuGeO_3 ¹, and theoretical calculations³ point toward a similar scenario in LiV_2O_5 . Doping with non-magnetic dopants is realized experimentally in CuGeO_3 by substituting a small fraction of copper atoms by zinc (or magnesium) atoms⁴. An intriguing low-temperature phase where antiferromagnetism coexists with the SP dimerisation was observed⁴. Similar doping-induced antiferromagnetic (AF) ordering has also been observed in the interacting dimer compound TiCuCl_3 ⁵. Theoretically, each dopant is expected to release a soliton which can be viewed as a single unpaired spin separating two dimer configurations⁶, hence leading to a rapid suppression of the spin gap under doping⁷. In an idealized spontaneously dimerised spin chain the soliton would not be bound to the dopant⁶. The physical picture is in fact completely different: A static bulk dimerisation is enforced by, e.g., couplings to the three-dimensional (3D) lattice, thus generating an attractive potential between the soliton and the dopant^{6,8}.

The dopant-soliton conformational mechanism is responsible for the formation of local $S=1/2$ magnetic moments^{6,9}. Within a realistic model including an elastic coupling to a two-dimensional (2D) lattice¹⁰, it was shown that these effective spins experience a non-frustrated interaction that could lead at $T=0$ to a finite staggered magnetization¹¹. Recently, similar conclusions were reached using a model with purely magnetic interactions including a four-spin exchange coupling¹². In this Letter, we analyze the formation of the dopant-induced AF order which coexists with the SP dimerisation. After using exact diagonalisation (ED) of small clusters (following Refs.^{11,12}) to construct an effective diluted $S=1/2$ model, we take advantage of the non-frustrated character of the resulting Hamiltonian to perform extensive

state-of-the-art stochastic series expansion (SSE) quantum Monte Carlo (QMC) simulations on 2D lattices as large as 288×288 with up to $N_s = 576$ (dopant) spins and down to temperature as low as $T = 1 = 2^{14}$ (or 2^{18} for $N_s = 256$). The uniform susceptibility is shown to exhibit a Curie-like behavior although the $T=0$ and infinite size extrapolated staggered magnetization is found to be finite down to the smallest dopant concentrations x available. The Neel temperature (assuming a small 3D coupling) is also computed versus x and compared to experiments.

We start with the microscopic Hamiltonian of a 2D array of coupled frustrated spin- $\frac{1}{2}$ chains and we summarize the procedure followed in Refs.^{11,12} to derive an effective Hamiltonian.

$$H = \sum_{i;a} [J(1 + \gamma_{i;a}) S_{i;a} \cdot S_{i+1;a} + J S_{i;a} \cdot S_{i+2;a} + h_{i;a} S_{i;a}^z]; \quad (1)$$

where the i and a indices label the L sites and M chains respectively. The energy scale is set by the exchange coupling along the chain ($J=1$) and γ is the relative magnitude of the next nearest neighbor frustrating magnetic coupling. Dopants are simply described as randomly located inert sites ($i;a$) (see Fig. 1) where $S_{i;a} = 0$ is set in Eq. (1). Small inter-chain couplings are included in a mean-field self-consistent treatment assuming,

$$h_{i;a} = J_2 (h S_{i;a+1}^z + h S_{i;a-1}^z); \quad (2)$$

$$i_{i;a} = \frac{J_4}{J} f h S_{i;a+1} \cdot S_{i+1;a+1} + h S_{i;a-1} \cdot S_{i-1;a-1} g; \quad (3)$$

While the first term accounts for first-order effects in the inter-chain magnetic coupling J_2 , the second term might have multiple origins; although a four-spin cyclic exchange mechanism provides the most straightforward derivation of it¹², at a qualitative level, J_4 can also mimic higher-order effects in J_2 ¹³ or the coupling to a 2D (or 3D) lattice. In that case, due to a magneto-elastic coupling, the modulations $i_{i;a}$ result from small displacements of the ions. The elastic energy is the sum of a

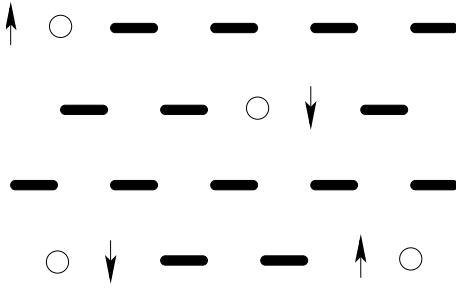


FIG. 1: Schematic picture of a doped SP system. Thick bonds correspond to dimers, and non-magnetic dopants (released spin- $\frac{1}{2}$) are represented by open circles (arrows).

local term $\frac{1}{2}K_k \sum_{i,j} \frac{1}{i-j} S_{i,j}^2$ and an inter-chain contribution $K_{\perp} \sum_{i,j} \frac{1}{i-j} S_{i,j}^2$ of electrostatic origin¹⁴. In that case Eq. (3) is replaced by¹⁰, $K_k \sum_{i,j} \frac{1}{i-j} S_{i,j}^2 + K_{\perp} \sum_{i,j} \frac{1}{i-j} S_{i,j}^2 = J_h S_{i,j}^2$, giving very similar results¹⁵ so that we shall restrict to Eq. (3) here.

By breaking a dimer, each dopant releases a soliton carrying a spin $1/2$. As shown previously¹², J_4 (or equivalently K_{\perp} in the alternative model¹⁰) leads to a confinement of the moment to the dopant with a localization length J_4 . At temperatures lower than the spin gap, these effective spins dominate the physics (see Fig.1) and a low-temperature description of the doped system can be obtained using an effective model including only (long-range) pairwise interaction between these local moments. The coupling J^e between two effective spins at arbitrary relative distance is computed by ED as the energy difference between their singlet and triplet configurations^{11,12}. The sign of this interaction (i.e. its ferromagnetic or AF nature) depends on whether the two dopants lie on the same or opposite sublattices¹⁶, so that an overall AF ordering is favored.

In order to derive an analytic expression for J^e valid at long distances, we fit the numerical ED data (restricted to short and intermediate length scales). A long-range non-frustrated Heisenberg model of diluted effective spin- $\frac{1}{2}$ can then be defined,

$$H^e = \sum_{r_1, r_2}^X J^e(r_1 - r_2) S_{r_1} \cdot S_{r_2}; \quad (4)$$

with $r_i = 1$ (0) with probability x ($1-x$), where x is the dopant concentration. Such a model can be studied by QMC on $L_x \times L_y$ clusters much larger than those accessible to ED¹¹ and at all temperatures. Using few phenomenological parameters, two energy scales and three length scales, simple expressions fit the ED data for a wide range of (physical) parameters. Naturally, one has to distinguish four cases depending on whether the dopants are located on the same ($a=0$) or on different chains, and whether they are located on the same or on different sublattices. When $a=0$ (same chain), J^e approximately fulfills $J^e(i;0) =$

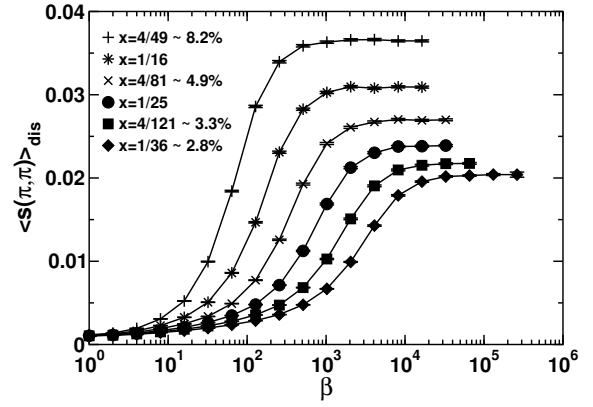


FIG. 2: Staggered magnetic structure factor per site vs inverse-temperature computed using a β -doubling scheme and averaged over 1000 to 2000 samples. Results for $N_s = 256$ spins on 56, 64, 72, 80, 88 and 96 (from top to bottom) lattices correspond to the concentrations x indicated on the plot.

$J_0(1 - \delta_{i,k})$ for i even and $i < k$ and otherwise $J^e(i;0) = 0$. For dopants located on different chains and on the same sublattice ($i+a$ even) one has, $J^e(i;a) = J_0^0 \exp(-\frac{i}{k}) \exp(-\frac{a}{\tau})$; while, if the dopants are on opposite sublattices, $J^e(i;a) = J_0^0 \frac{1}{2} \exp(-\frac{a}{\tau})$ for $i < 2k$ and $J^e(i;a) = J_0^0 \exp(-\frac{i-2k}{k}) \exp(-\frac{a}{\tau})$ for $i > 2k$. The fitting parameters used here for $\tau = 0.5$, $J_2 = 0.1$ and $J_4 = 0.08$ are $J_0 = 0.52$, $J_0^0 = 0.3$, $\frac{1}{k} = 17.3$, $\frac{1}{k} = 2.5$ and $\tau = 1$. We stress that the alternating sign of J^e is a crucial feature of the interaction which guarantees the absence of frustration. Note also that the magnitude of J^e shows a unique exponential behavior $\sim \exp(-\frac{i}{k} - \frac{a}{\tau})$ at long distance although its short distance behavior is more complicated (but probably not relevant). The distribution of these coupling contains a very large density of couplings of small magnitudes.

We study the effective Heisenberg model using the SSE method¹⁷ to investigate GS as well as finite T properties. In this approach, the interactions are sampled stochastically, and for a long-ranged interaction the computational effort is then reduced from N_s^2 to $N_s \ln(N_s)$ ¹⁸. In order to accelerate the convergence of the simulations at the very low temperatures needed to study the ground state, we use a β -doubling scheme¹⁹ where the inverse temperature is successively increased by a factor 2. Comparing results at several $\beta = 2^n$, one can subsequently check that the $T \rightarrow 0$ limit has been reached.

The AF ordering instability is signalled by the divergence with system size of the staggered structure factor,

$$S(\vec{q}) = \frac{1}{L_x L_y} \sum_i h(\vec{q} \cdot \vec{r}_i) S_i^z; \quad (5)$$

Note that within our effective model approach, only the

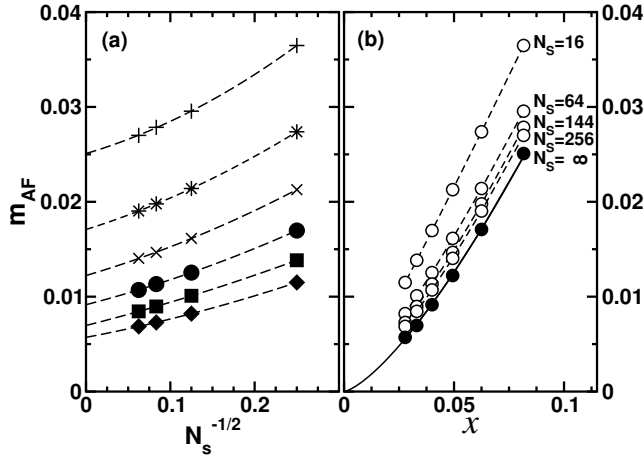


FIG. 3: Staggered magnetization per site. Disorder average has been done over at least 2000 samples. (a) Finite size extrapolations (see text) at fixed doping x . The symbols are identical to Fig. 2 for x varying from 2.8% to 8.2%. (b) Doping dependence of m_{AF} for various numbers of spins and in the thermodynamic limit (full symbols).

sites carrying a "dopant spin" contribute to this sum. It is convenient to normalize S with respect to the number of sites, i.e. to define a staggered structure factor per site; $s(\mathbf{r}; \mathbf{r}') = S(\mathbf{r}; \mathbf{r}')/L_x L_y$. In an ordered AF state, $s(\mathbf{r}; \mathbf{r}')$ should converge, with increasing size, to a non-zero value $< 1/4$. The (finite size) sublattice magnetization m_{AF} can then be obtained by averaging $s(\mathbf{r}; \mathbf{r}')$ over a large number of dopant distributions, i.e. $\langle m_{AF} \rangle^2 = 3 \langle s(\mathbf{r}; \mathbf{r}') \rangle_{dis}^2$, where the factor 3 comes from the spin-rotational invariance²⁰ and $\langle \cdot \rangle_{dis}$ stands for the disorder average. The staggered magnetization per dopant is then simply $m_{spin} = m_{AF}/x$. We have checked that extrapolations to the thermodynamic limit using different aspect ratios L_y/L_x give similar results and, here, we only report data for $L_y = L_x = L$.

Since, strictly speaking, in 2D the divergence of $S(\mathbf{r}; \mathbf{r}')$ occurs only at $T = 0$ ($\chi = 1$) it is appropriate to first extrapolate the finite size numerical data to $T = 0$. As shown in Fig. 2 the staggered structure factor saturates at sufficiently low temperature and the GS value of m_{AF} (averaged over disorder) can be safely obtained. Then, using a polynomial fit in $1/N_s$ (order 2 is sufficient) an accurate extrapolation to the thermodynamic limit, $N_s \rightarrow \infty$ (or $L \rightarrow \infty$ at constant x), is performed as shown in Fig. 3 (a). The doping dependence of the extrapolated m_{AF} is given in Fig. 3 (b). Note that our results, although consistent with previous ($T = 0$) extrapolations attempted on small clusters¹¹, are far more accurate due to the use of much larger systems. We have tested various fits to the data. Assuming a power law $m_{AF} \propto x^\alpha$, the best fit (solid line in Fig. 3 (b)) gives an exponent $\alpha = 1.38 > 1$. However, the alternative behavior $a_1 x + a_2 x^2$ would only be distinguishable at even smaller x .

We have computed the uniform susceptibility $\chi(T)$ for

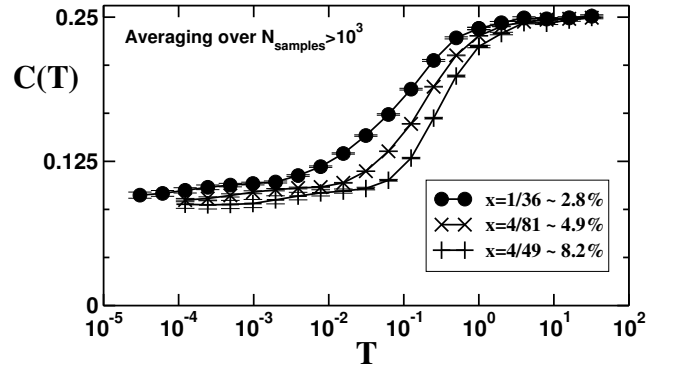


FIG. 4: Curie constant $C(T)$ vs T shown for $N_s = 144$ spins and 3 different concentrations x (as shown on plot).

a wide range of temperatures. Results for the Curie constant $C(T) = T \chi(T)$ are shown in Fig. 4. At the highest temperatures the effective dopant spins behave as free spins while at low temperature we observe a new Curie-like behavior with a reduced Curie constant $\chi = 1/2$. Although here the 2D system orders at $T = 0$ (as proven above) this behavior agrees with a qualitative argument by Sigrist and Furusaki⁶ based on the formation of large spin clusters. A detailed analysis of a low-temperature scaling regime similar to the one observed in random ferromagnetic-antiferromagnetic spin chains²¹ will be reported elsewhere²³.

We finish this investigation by calculating the Neel temperature, assuming a small (effective) 3D magnetic coupling J_{3D} between the 2D planes. Using an RPA criterion, the critical temperature T_N is simply given by $\chi_{stag}(T_N) = 1/J_{3D}$ where the staggered spin susceptibility (normalized per site) is defined as usual by,

$$\chi_{stag}(T) = \frac{1}{L^2} \sum_{i,j} \langle S_i^z S_j^z \rangle = \frac{1}{L^2} \sum_{i,j} \langle S_i^z S_j^z \rangle_0 S_j^z(0) S_i^z(0); \quad (6)$$

and averaged over several disorder configurations (typically 2000). Since $\chi_{stag}(T_N)$ is expected to reach its thermodynamic limit for a finite linear size L as long as T_N remains finite, accurate values of T_N can be obtained using a finite size computation of $\chi_{stag}(T)$ for not too small inter-chain couplings. Fig. 5 (a) shows that $\chi_{stag}(T)$ diverges when $T \rightarrow 0$. T_N is determined by the intersection of the curve $\chi_{stag}(T)$ with a horizontal line at coordinate $1/J_{3D}$. Note that finite size corrections remain small, even in the worst case corresponding to very small J_{3D} values and large dopant concentrations. The doping dependence of T_N is plotted in Fig. 5 (b) for a particularly small value $J_{3D} = 0.01$ (in order to show the small size dependence observable in that case). It clearly reveals a rapid decrease of T_N when $x \rightarrow 0$, but, in agreement with experiments, does not suggest a non-zero critical concentration. In Fig. 5 (b), we show the behavior of $T_N(x)$ down to $x \approx 0.007$. Note that from numerical fits of our data, we can not clearly distinguish between a power-law be-

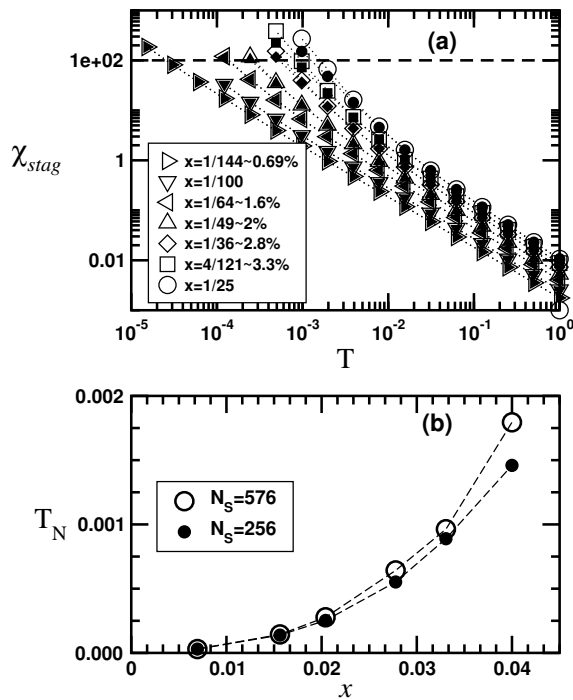


FIG. 5: (a) Staggered susceptibility of a 2D layer vs temperature (using log-log scales) for $N_s = 256$ (full symbols) and $N_s = 576$ (open symbols) spins. Concentrations x are shown on the plot (similar symbols as in Figs. 2 and 3). $3D = 100$ is shown by the dashed line. (b) Neel temperature vs dopant concentration x for a 3D RPA inter-plane coupling $3D = 0.01$ and for $N_s = 256$ and $N_s = 576$ spins.

havior (with an exponent -2.5) and an exponential law like $A \exp(-B/x)$, as suggested by fits of experimental data for $\text{Cu}_{1-x}\text{Zn}_x\text{GeO}_3$ ²².

In summary, we have studied an effective low-energy Hamiltonian (valid for low temperature physics) describing the interaction of a finite concentration of spinless dopants randomly distributed in a generic low-dimensional (frustrated) SP system. The SSE method, which is applicable here because of the non-frustrated nature of the effective model, was used in combination with finite-size scaling to compute both GS and finite temperature properties. The uniform susceptibility exhibits a Curie-like behavior down to very low temperature. We also predict that the AF order develops continuously without any finite critical dopant concentration in agreement with experiment.

AW S acknowledges support from the Academy of Finland, project NO. 26175. DP thanks M. Sigrist for pointing out that the uniform susceptibility data could be interpreted as a scaling regime. Further investigations along these lines are under way²³. We thank IDRIS (Orsay, France) for using their supercomputer facilities.

- ¹ M. Hase, I. Terasaki, and K. Uchinokura, Phys. Rev. Lett. 70, 3651 (1993).
- ² M. Isobe and Y. Ueda, J. Phys. Soc. Jpn. 65, 3142 (1996); R. Valentiet al., Phys. Rev. Lett. 86, 5381 (2001).
- ³ F. Becca, F. Mila and D. Poilblanc, Phys. Rev. Lett. 91, 067202 (2003).
- ⁴ M. Hase et al., Phys. Rev. Lett. 71, 4059 (1993); S. B. Osero et al., Phys. Rev. Lett. 74, 1450 (1995); L. P. Regnault et al., Europhys. Lett. 32 579 (1995); T. Masuda et al., Phys. Rev. Lett. 80, 4566 (1998); B. Grenier et al., Phys. Rev. B 58, 8202 (1998).
- ⁵ A. Oosawa, T. Ono, and H. Tanaka, Phys. Rev. B 66, 020405 (2002).
- ⁶ E. S. Srensen, I. A. A. Eck, D. Augier, and D. Poilblanc, Phys. Rev. B 58, R14701 (1998).
- ⁷ G. B. Martins, E. Dagotto and J. Riera, Phys. Rev. B 54, 16032 (1996).
- ⁸ T. Nakamura, Phys. Rev. B 59, R6589 (1999).
- ⁹ B. Normand and F. Mila, Phys. Rev. B 65, 104411 (2002).
- ¹⁰ P. Hansen, D. Augier, J. Riera, and D. Poilblanc, Phys. Rev. B 59, 13557 (1999).
- ¹¹ A. Dobry et al., Phys. Rev. B 60, 4065 (1999).
- ¹² N. Laorencie and D. Poilblanc, Phys. Rev. Lett. 90, 157202 (2003).
- ¹³ Chains with in-phase relative dimerisations are stabilized by an energy $\propto J_2^2/J$ (per bond) w.r.t. the alternating configuration; see T. M. R. Byrnes, M. T. Murphy and O. P. Sushkov, Phys. Rev. B 60, 4057 (1999).
- ¹⁴ I. A. A. Eck, Proceedings of the NATO ASI: Dynamical properties of Unconventional Magnetic Systems, April 1997, cond-mat/9705127 (unpublished).
- ¹⁵ In fact, for the undoped system, an exact mapping exists assuming $2J_4 = J = J = K_e$ where $K_e = K_k - 2K_{\pi/2}$.
- ¹⁶ For related studies of a doped spin ladder with no frustration see M. Sigrist and A. Furusaki, J. Phys. Soc. Jpn 65, 2385 (1996).
- ¹⁷ A. W. Sandvik, Phys. Rev. B 59, R14157 (1999).
- ¹⁸ A. W. Sandvik, Phys. Rev. E 68, 056701 (2003).
- ¹⁹ A. W. Sandvik, Phys. Rev. B 66, 024418 (2002).
- ²⁰ J. D. Reger and A. P. Young, Phys. Rev. B 37, 5978 (1988).
- ²¹ E. W. Estenberg, A. Furusaki, M. Sigrist and P. A. Lee, Phys. Rev. Lett. 75, 4302 (1995); B. Frischmuth and M. Sigrist, Phys. Rev. Lett. 79, 147 (1997); B. Frischmuth et al., Phys. Rev. B 60, 3388 (1999).
- ²² K. M. Anabe et al., Phys. Rev. B 58, R575 (1998).
- ²³ N. Laorencie, D. Poilblanc, A. Sandvik and M. Sigrist, in preparation.

